Spin-glass behavior of the antiferromagnetic Ising model on a scale-free network

M. Bartolozzi,[1,*] T. Surungan,[1,2,†] D. B. Leinweber,[1,‡] and A. G. Williams[1,§]
[1]*Special Research Center for the Subatomic Structure of Matter (CSSM), The University of Adelaide, Adelaide, SA 5005, Australia*
[2]*Department of Physics, Hasanuddin University, Makassar 90245, Indonesia*
(Received 20 December 2005; published 15 June 2006)

Antiferromagnetic Ising spins on the scale-free Barabási-Albert network are studied via the Monte Carlo method. Using the replica exchange algorithm, we calculate the temperature dependence of various physical quantities of interest including the overlap and the Binder parameters. We observe a transition between a paramagnetic phase and a spin-glass phase and estimate the critical temperature for the phase transition to be $T\sim 4.0(1)$ in units of J/k_B, where J is the coupling strength between spins and k_B is the Boltzmann constant. Using the scaling behavior of the Binder parameter, we estimate the scaling exponent to be $\nu\sim 1.10(2)$.

DOI: 10.1103/PhysRevB.73.224419 PACS number(s): 89.75.Hc, 75.10.Nr, 64.60.Cn, 05.70.Fh

I. INTRODUCTION

In the last few years, the study of complex networks has found relevance in various fields including sociology, ecology, biology, economics, and physics. In these networks, vertices do not have homogeneous links or connectivities. A particularly relevant structure found in several empirical studies is the so-called *scale-free network* (SFN), which is characterized by the power-law distribution of the degree of connectivities, $P(k)\sim k^{-\gamma}$, with k the number of links for a node, and γ the decay exponent of the distribution. A network with $\gamma\rightarrow 0$ has nodes with a relatively homogeneous number of links (somewhat resembling the case on regular lattices), while large γ corresponds to the existence of "very famous" nodes (or hubs), i.e., those having direct links to the majority of vertices.

Many networks realized in nature show scale-free structure. Some examples studied include food webs,[1] power grids and neural networks,[2,3] cellular networks,[4] sexual contacts,[5] Internet routers,[6] the World Wide Web,[7] actor collaborations,[2,3,8,9] the citation network of scientists,[10] and the stock market.[11]

In addition to the scale-free behavior, these networks are characterized by a high clustering coefficient, C, in comparison with random graphs.[12] The clustering coefficient, C, is computed as the average of local clustering, C_i, for the ith node, defined as

$$C_i = \frac{2y_i}{z_i(z_i-1)}, \tag{1}$$

where z_i is the total number of nodes linked to the site i and y_i is the total number of links between those nodes. As a consequence both C_i and C lie in the interval $[0,1]$. The high level of clustering found supports the idea that a *herding* phenomenon is a common feature in social and biological communities. The parameter C also represents the density of triangles, that is of elementary cells, associated with the network.

Numerical studies on SFNs have demonstrated how topology plays a fundamental role in infection spreading,[13] opinion formation in large communities,[14] and tolerance against random and preferential node removal.[14,15] A detailed description of the progress in this emerging field of statistical mechanics can be found in the recent reviews of Refs. 16–18.

The aforementioned empirical findings have inspired physicists to investigate the dynamics of standard models in the new case where the interactions between elements are described by complex networks. These include the study of various magnetic models such as the Ising model. An intriguing issue concerns how the unusual topology acts to influence the cooperative behavior of the spins. Studies of the ferromagnetic (FM) Ising model on a SFN, using several theoretical techniques[19–22] including the Monte Carlo (MC) method,[22] have found the robustness of ferromagnetic ordering against thermal fluctuations for the degree distribution exponent $\gamma\leqslant 3$. This result is actually intuitive if we notice that, as γ gets smaller, nodes at the edge of the network will generally have more connections. In this situation, the system resembles the FM Ising model on a regular lattice which exceeds the lower critical spatial dimension, $d_l=2$. There the ordered phase is very robust against thermal fluctuations. However, for the antiferromagnetic (AF) case with a SFN, the situation is different.

Two factors come to play a central role in the dynamics of the AF-SFN model; namely the competition induced by the AF interaction in the elementary triangles of the network and the randomness related to the nonregular connections. The abundance of elementary triangles in the network leads to frustration, as, for example, only two of the three spins can be anti-aligned. More generally, frustration refers to the inability of the system to remain in a single lowest energy state (ground state). These ingredients lead the AF SFN to belong to a class of randomly frustrated systems commonly referred to as spin glasses (SGs).

Most studies of SGs have been performed on regular lattices. These studies have shown that frustration and randomness are the key ingredients for SG behavior, characterized by a frozen random spin orientation at low temperatures.[23] Spin glasses on a SFN with mixed AF and FM bonds have been investigated recently by Kim *et al.*[24] They found, for $\gamma\leqslant 3$ and even distributions of the two kinds of interaction, that the system is always in a SG state for any finite temperature. A study of the pure AF Ising model on a SFN is of great theoretical interest since, despite the homogeneity of the bonds, it inherits all the characteristics of a SG from the

random frustration related to its geometry. General reviews on SG systems can be found in Ref. 23.

In this paper we consider the AF Ising model on a SFN, more precisely the Barabási-Albert (BA) network with tunable clustering.[25] Using the replica exchange algorithm[26] of the Monte Carlo method, we calculate the order parameters of spin-glass behavior, the so-called overlap parameter, and its distribution. For an accurate determination of the critical temperature, we also evaluate the Binder parameter. The paper is organized as follows: Sec. II describes the model and the method. The results are discussed in Sec. III. Section IV is devoted to the concluding remarks.

II. MODEL AND SIMULATION METHOD

A. The model

In order to create the scale-free network topology we make use of the Barabási-Albert model.[9] This is based on two main considerations: (i) linear growth and (ii) preferential attachment. In practice the network is initialized with m_0 disconnected nodes. At each step a new node with m edges is added to the preexisting network. The probability that an edge of the new node is linked with the ith node is expressed by $\Pi(k_i)=k_i/\Sigma_j k_j$. The iteration of this preferential growing process yields a scale-free network, where the probability of having a node with k connections is $P(k)\sim k^{-\gamma}$ with $\gamma=3$. This is an interesting value. In the thermodynamic limit, the second moment of the distribution diverges, $\langle k^2\rangle=\infty$, for $\gamma \leqslant 3$. This leads to peculiar properties of theoretical models in this range of γ values.[18] In the present work we focus on the case in which $\gamma=3$ and the divergence of $\langle k^2\rangle$ is logarithmic. An extensive investigation of the phase space for the AF model on SFN is left for future work.

It is also worth noting that the Barabási-Albert model cannot reproduce a high clustering coefficient. In fact, the value of this coefficient depends on the total number of nodes, N, in the network[16] and in the thermodynamic limit, $N\to\infty$, $C\to 0$.

In the AF Ising system the average cluster coefficient, C, plays a fundamental role in the dynamics. In fact, it represents the average number of triangles per node and, as a result, it is directly related to the degree of frustration in the network. In order to keep this parameter constant, on average, with the size of the network, we introduce a further step in the growth process, namely the triad formation proposed by Holme and Kim.[25] In this case, if the new added node is linked with an older node, i, having other links, then with a certain probability, θ, the next link of the new node, if any remain, will be added to a randomly selected neighbor of node i. This method of introducing friends to friends, while preserving the scale-free nature of the networks with $\gamma\sim 3$, generates high clustering coefficients that do not depend on N. The only tunable parameter that changes the value of the clustering coefficient is the *clustering probability* θ. An example of a SF network generated with this algorithm is shown in Fig. 1 for 500 nodes.

We simulate various sizes of the network with many different realizations and investigate the scaling behavior of the various physical quantities we are interested in. All the simulations have been carried out fixing $\theta=0.9$, corresponding to an average clustering coefficient of $C\sim 0.39$, close to the value found in many real systems.[16] On each SFN constructed at the beginning of the simulation, we assign to each vertex an Ising spin, and to each link an AF interaction. The Hamiltonian can be written as follows:

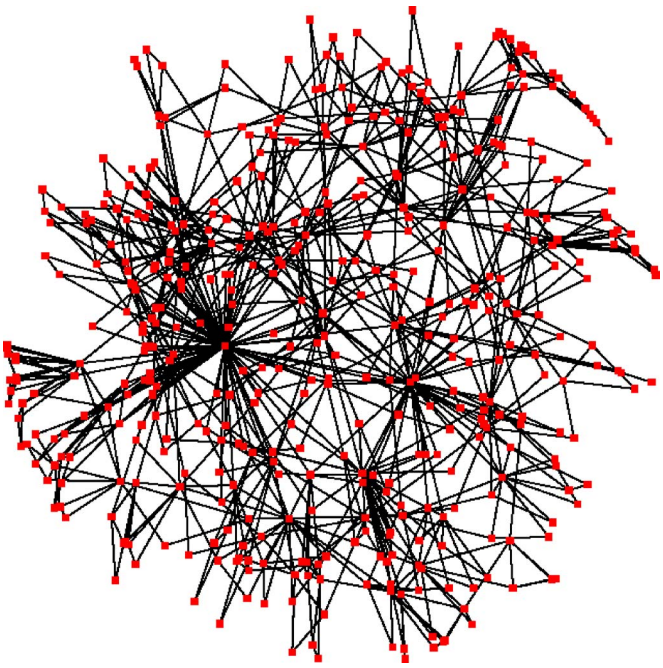

FIG. 1. (Color online) Example of a scale-free network. The number of nodes is 500 with clustering probability $\theta=0.9$ and $m_0=m=2$. The number of nodes has been kept small in order to preserve the clarity of the plot. Note that, for such small networks, a large scale invariant range is obtained only if one considers the ensemble average over several realizations. This plot has been realized with the Pajek software (Ref. 27).

$$H=-\sum_{\langle ij\rangle} J_{ij}s_i s_j. \tag{2}$$

Here the summation is performed over the connected spins s_i and s_j occupying sites i and j, respectively. The coupling interaction $J_{ij}=J=-1$ is AF. As previously mentioned, each vertex with the local cluster coefficient $C_i>0$ together with its neighbors, composes elementary triangles. Due to the AF interactions the local system is frustrated.

It is worth pointing out that C is related to the degree of frustration of each network. Due to the probabilistic algorithm used for their construction, the value of C fluctuates around a mean value from one network to the next and, therefore, provides a source of randomness that, as we will see, gives rise to the spin glass properties of the model. This probabilistic growth is not shared by other algorithms which use recursion formulas to generate scale-free structures, such as, for example, the Apollonian networks.[28] In this case, once one fixes the number of iterations of the algorithm, which is proportional to the number of nodes of the final network, one

also fixes its topology. The element of randomness is therefore missing in the Apollonian procedure.

As a random system, each realization of a network of size N will differ in the "structure" of connectivities. Therefore, in order to have reliable statistics, we average over many realizations of the SF network for each specified size. The system sizes that we simulate are $N=1024$, 2048, 4096, and 8192. In general, one takes into account more realizations for small system sizes and less for large system sizes as the latter tend to self-average. However, since the self-averaging of physical quantities for larger system sizes is interfered with by the increase of ground state degeneracy, we do not take less realizations. Instead all physical quantities of interest for each system size are averaged over 1000 network realizations. Moreover, for each realization of the network, we fix $m_0=m=5$, corresponding to a coordination number on a regular lattice of approximately 10. In the thermodynamic limit, the average connectivity for the BA network is $\langle k\rangle = 2m=10$, emphasizing the fact that we are implicitly dealing with a high dimensional system.

Another peculiarity of SF networks is the existence of a broad distribution of "hubs," that is nodes with a large number of connections, k. The energy difference in a spin flip actually depends on the number of connections of the spin itself, $\Delta E_i=-2s_i\Sigma_{j=1}^{k_i}s_j$. Thus in the AF case for the ith spin with k_i connections, the hubs are more likely to "freeze" into a particular configuration compared to the nodes with just a few links. This property resembles the spin-glass behavior of particular alloys where some elements freeze into a particular orientation at a higher temperature than others.

B. Simulation method

The calculation of the thermal averages of the physical quantities of interest is performed using the replica exchange MC method.[26] In this method the evolution of M replicas, each in equilibrium with a heat bath of inverse temperature β_m for the mth replica, is simulated in parallel. Given a set of inverse temperatures, $\{\beta\}$, the probability distribution of finding the whole system in a state $\{X\}=\{X_1,X_2,\ldots,X_M\}$ is

$$P(\{X,\beta\}) = \prod_{m=1}^{M} \tilde{P}(X_m,\beta_m), \tag{3}$$

with

$$\tilde{P}(X_m,\beta_m) = Z(\beta_m)^{-1}\exp[-\beta_m H(X_m)], \tag{4}$$

and $Z(\beta_m)$ is the partition function at the mth temperature. We can then define an exchange matrix between the replicas in our Markov chain, $W(X_m,\beta_m|X_n,\beta_n)$, that is the probability to switch the configuration X_m at the temperature β_m with the configuration X_n at β_n. By using the detailed balance condition, required to keep the entire system at equilibrium, on the transition matrix

$$\begin{aligned} &P(\ldots,\{X_m,\beta_m\},\ldots,\{X_n,\beta_n\},\ldots)W(X_m,\beta_m|X_n,\beta_n) \\ &= P(\ldots,\{X_n,\beta_m\},\ldots,\{X_m,\beta_n\},\ldots)W(X_n,\beta_m|X_m,\beta_n), \end{aligned} \tag{5}$$

along with Eq. (4), we have that

$$\frac{W(X_m,\beta_m|X_n,\beta_n)}{W(X_n,\beta_m|X_m,\beta_n)} = \exp(-\Delta), \tag{6}$$

where $\Delta=(\beta_n-\beta_m)[H(X_m)-H(X_n)]$. With the above constraints we can choose the matrix coefficients according to the standard Metropolis method and, therefore, we have

$$W(X_m,\beta_m|X_n,\beta_n) = \begin{cases} 1 & \text{if } \Delta<0, \\ \exp(-\Delta) & \text{if } \Delta>0. \end{cases} \tag{7}$$

In our simulation we restrict the exchange to temperatures next to each other; that is, we consider only the terms $W(X_m,\beta_m|X_{m+1},\beta_{m+1})$. This choice is motivated by the fact that the acceptance ratio decays exponentially with $(\beta_n-\beta_m)$.

The replica exchange method is extremely efficient for simulating systems such as spin glasses, that can otherwise become frozen in some particular configuration at low temperatures when using a standard Metropolis algorithm for the configuration update. In this case, as we lower the temperature, the system can become trapped into a local minimum of the free energy where the barriers are so high that the time required for the system to move to another allowed region of the configuration space diverges to infinity as a function of the system size. If the system is trapped in a local minimum then the ergodicity condition is not fulfilled anymore and the measure that one makes becomes biased by the particular region of the configuration space that is being sampled. By using the exchange replica method, instead, we keep switching the temperatures between the M copies of the system and, as long as the higher temperature is in a hot phase (where the system can easily explore all the configuration space), then we are in principle able to explore all the configuration space also for the lower temperatures. Another advantage of this method is that the replica exchange reduces drastically the temporal correlation in the system dynamics at each temperature. This enables one to collect more independent measures for the thermal averages of the physical quantities and, therefore, reduces the uncertainty.

It is important to stress that, before starting the actual simulations, some care is required in selecting the set of inverse temperatures, $\{\beta\}$. In fact, the method is efficient only when a fairly large transition probability is maintained in the range of interest. From Eq. (7), we can see that, in the hot phase, temperatures can be more coarsely spaced while in the cold phase the temperatures need to be closer to each other. An optimal set of temperatures can be obtained by iterating, in preliminary runs, the following map:[26]

$$\begin{aligned} \tilde{\beta}_1 &= \beta_1, \\ \tilde{\beta}_m &= \tilde{\beta}_{m-1} + (\beta_m - \beta_{m-1})p_m/c, \end{aligned} \tag{8}$$

where p_m is the acceptance ratio for the switch between two configurations at the mth temperature and $c=\Sigma_{m=1}^{M}p_m/(M-1)$ is a normalization factor. The initial value for the set $\{\beta\}$ is uniform in the interval of interest and we ensure that β_1 belongs to the hot phase. For each iteration of the map, a run of a few thousand MC steps is carried out to calculate the acceptance ratios, p_m, which are then plugged into Eq. (8) in

order to obtain a new set of inverse temperatures. After a few iterations, the map of Eq. (8) converges to a fixed point, $\{\beta^*\}$, which sets the values of the temperatures to be used in our simulations.

In using this method, we define a "local" MC (LMC) update as a MC update for each spin of each replica, either consecutively through all elements of the network or randomly. Given that we can group the inverse temperatures in even and odd pairs, (β_m, β_{m+1}), after each LMC update we alternate attempts to switch configurations from one temperature to the next. According to this procedure, we define a Monte Carlo step (MCS) as a LMC plus a half (m odd or even) exchange trial.

For each realization of the network we start from a random configuration of the spins and then perform 10^3 LMC updates in order to reach thermal equilibrium. After this transient period, we run the simulation for 3×10^5 MCSs while taking a total of 6×10^4 measures for the thermal averages, that is one every 5 MCSs (temporal correlations are lost very quickly by using the replica exchange method). We consider low temperatures in a search for the possible existence of a phase transition. The thermal averages obtained for each network are then averaged over the ensemble of networks. In the following, we indicate $\langle\cdots\rangle$ as the thermal average and $[\cdots]_{\text{av}}$ as the ensemble average. The statistical errors in the plots, where reported, are calculated via the bootstrap method.

III. RESULTS AND DISCUSSION

A. Spatial correlations and specific heat

As a first step we investigate the extent of spatial correlation of the spins in the SF network by making use of the spatial autocorrelation function which is defined on a regular lattice as

$$\xi(r) = \left[\frac{1}{L_d}\langle s_i s_{i+r}\rangle\right]_{\text{av}}, \tag{9}$$

where L_d is the total number of pairs at distance r and depends just on the dimension considered. In a SF network the situation is more complicated since there may be several paths leading from a certain node to another. We then define r as the *minimum* path between two nodes and the denominator of Eq. (9) becomes dependent on r. The results, averaged over 50 configurations, between the temperatures of $T=5.0$ and 2.1 are shown in Fig. 2 for $N=1024$. All the temperatures in the present paper are expressed in units of J/k_B, where J is the coupling strength between spins and k_B is the Boltzmann constant.

In order to give a better interpretation of the plot in Fig. 2 we remind the reader about an important propriety of SF networks; that is their "small world structure." The "hubs," in fact, play a fundamental role in linking sites otherwise very distant. Moreover, the average path length increases just logarithmically with the size of the network.[16,17] In the plot of Fig. 2, for $N=1024$ nodes, an upper limit of $r=6$ is encountered. While all the 50 configurations reach $r=6$, only a few networks exceed this limit.

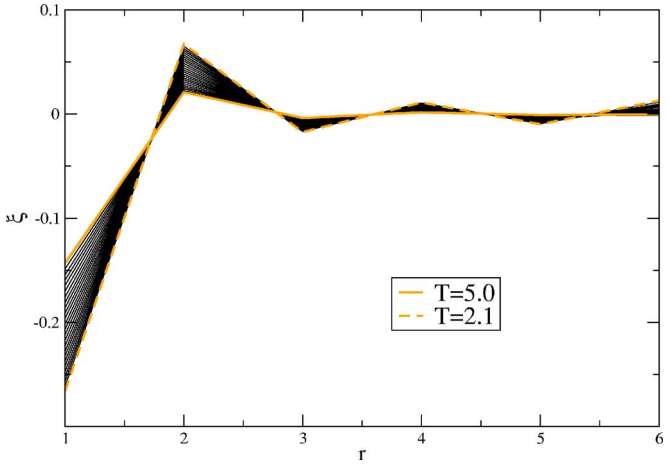

FIG. 2. (Color online) Spatial autocorrelation, $\xi(r)$, for $N=1024$ averaged over 50 network configurations for temperatures between $T=5.0$ and 2.1. The plot shows that next neighbor spins tend to be antiparallel as in the standard AF Ising model. The AF interaction in the triangular units of the system results in high frustration. Note that the number of nodes at large distances is much smaller than the ones at smaller distances and so the average calculated for $r=5$ and $r=6$ includes just a few samples. This is a consequence of the "small-world" effects in SF networks.

The plot emphasizes how neighboring spins, on average, tend to be anticorrelated, as expected in the AF case. The autocorrelation decreases with the distance from the node under consideration. The temperature dependence is also in accord with the expectations. The absolute value of the correlation decreases with increasing temperature and vice versa. Indeed, the highest and lowest temperatures form a perfect boundary for all the curves. This is an expected result, since thermal effects always tend to reduce the correlation between the spin interactions.

We also study the behavior of the specific heat, C_ν, defined as follows:

$$C_\nu(T) = \left[\frac{1}{Nk_BT^2}(\langle E^2\rangle - \langle E\rangle^2)\right]_{\text{av}}, \tag{10}$$

where k_B is the Boltzmann constant. Although no singularity is expected for this quantity in the spin-glass transition, it is interesting to compare its behavior with other studies. The dependence of the specific heat on temperature is reported in Fig. 3. The statistical errors, in this case, are smaller than the size of the symbols and therefore are not reported. A common Schottky peak of the specific heat for a finite system is observed at the temperature of $T\sim2.0$ independent of the system size. Below this point, we found that C_ν decreases and goes to zero as $T\to0$.

This behavior follows from simple entropy considerations. In fact, since we are dealing with a finite Ising system, the entropy is bounded at each finite temperature as well,

$$S(T) = \int_0^T \frac{C_\nu(T)}{T}dT < 2^N, \tag{11}$$

and, necessarily, $C_\nu\to0$ for $T\to0$.

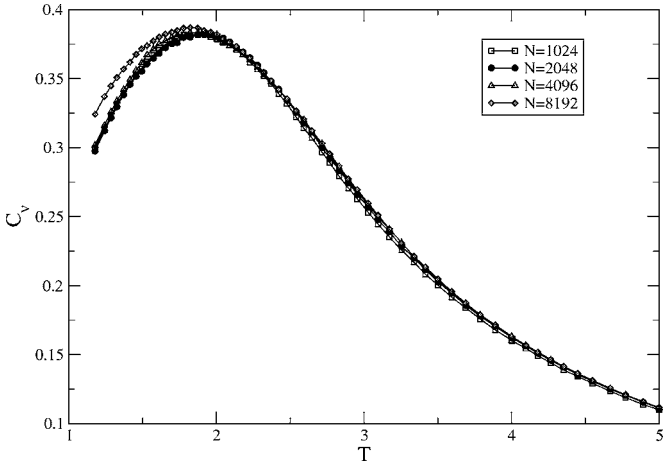

FIG. 3. Specific heat, C_v, as a function of the temperature and system size. The plot has been obtained by averaging over 50 network configurations for each N. Note that the specific heat does not scale with the size of the system.

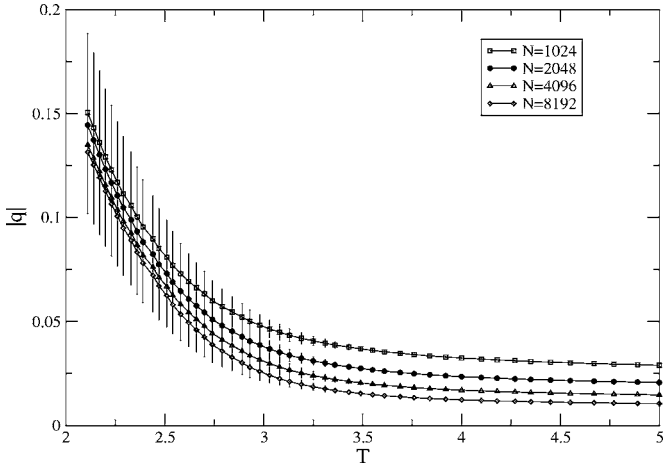

FIG. 4. Temperature dependence of the overlap parameter, q, for different system sizes N. The increasing value of q at low temperatures indicates a SG phase. For a given network size, 1000 realizations of the SFN are averaged over.

The next section is dedicated to study of the SG behavior and the phase transition of the system. In order to achieve this task, we evaluate the corresponding order parameters, the overlap parameter, and the Binder parameter.

B. Observing spin-glass behavior

With the presence of frustration and randomness in the AF-SFN model, we expect to observe a spin-glass transition, i.e., a transition from a temporal disordered to a temporal ordered phase at low temperatures.

This feature is not shared by the so-called fully frustrated systems.[29] This type of transition might be characterized by the order parameter such as that suggested by Edward and Anderson,[30] defined as follows:

$$q_{EA} = \left[\frac{1}{N} \sum_i \langle s_i \rangle^2 \right]_{\text{av}}. \tag{12}$$

However, an ergodic Markov chain of a system having Z_2 symmetry will ensure the thermal average of the ith spin vanishes. Therefore a finite value of this measure simply reflects the nonergodicity in the MC update.

A more appropriate quantity that is often used to characterize the SG state is the overlap parameter, q, defined as[31,32]

$$q = \frac{1}{N} \sum_i s_i^{(\alpha)} s_i^{(\beta)}, \tag{13}$$

where the superscripts α and β denote two copies of the same configuration of connectivity at the same temperature. The actual value of q is extracted from both the thermal and disorder average, $[\langle \cdots \rangle]_{\text{av}}$.

Using the replica exchange MC simulation, the two copies, α and β, are allocated at each temperature of the parallel tempering. This means, if the measurement is performed on M points of temperatures, there are M pairs of replicas. The Metropolis spin update is performed on each node for every MC step. As a part of the equilibration steps of the algorithm described in the previous section, we exchange two α (and β) replicas of neighboring temperatures, according to a certain probability. Then, for each temperature, the α and β replicas are superimposed every 5 MCSs in order to measure the overlap parameters, as defined in Eq. (13).

In particular, for the Ising system, due to the Z_2 symmetry, it is important to evaluate the absolute value of the order parameter,

$$|q| \equiv \left[\left\langle \left| \frac{1}{N} \sum_i s_i^{(\alpha)} s_i^{(\beta)} \right| \right\rangle \right]_{\text{av}}, \tag{14}$$

to overcome the implication of the Z_2 symmetry of the Hamiltonian, that is the configurations s_i and $-s_i$ have equal Boltzmann weights. That is, if the system is at thermal equilibrium and if we take quite long MCS then the usual q should average to zero. The existence of a spin-glass phase is indicated by the convergence of $|q|$ to a finite value as we increase the network size. At the same time, a convergence of $|q|$ to zero at high temperatures is anticipated. In the latter case the system is in the paramagnetic phase.

The temperature dependence of $|q|$, resulting from the simulations, is shown in Fig. 4. The existence of a SG phase is indicated by the finite value of $|q|$ in the low temperature region, and the approach of $|q|$ to zero at higher temperatures associated with the paramagnetic phase. For high temperatures and large networks, $|q|$ is approaching zero in accord with the thermodynamic limit where $|q| = 0$.[33]

The existence of these two different phases can also be observed from the distribution of q, as shown in Fig. 5. For higher temperatures we observe simple Brownian fluctuations of the values of q, leading to a singly peaked Gaussian distribution characteristic of a paramagnetic state. By decreasing the temperature, the distribution spreads out, reflecting the increasing number of metastable disordered states associated with a substantial frustration. At lower temperatures the distribution develops double peaks reflecting the Z_2 symmetry and a finite value of $|q|$, representative of the SG

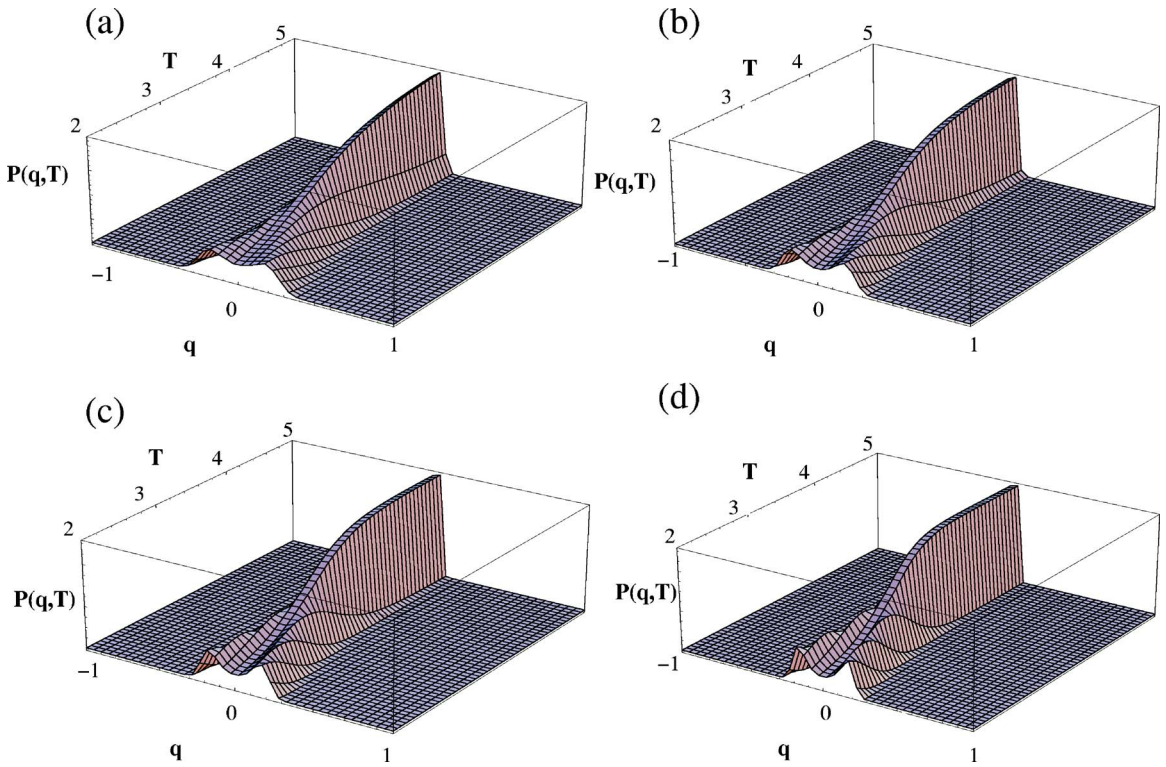

FIG. 5. (Color online) The distribution of q at various temperatures for different system sizes, including (a) $N=1024$, (b) $N=2048$, (c) $N=4096$, and (d) $N=8192$.

phase. We note that the shape of the observed distribution at low temperatures is different from that of the conventional Ising system where the double peaks approach deltalike double peaks reflecting a simple doubly degenerate ground state.[34]

An accurate evaluation of critical temperature of the phase transition is achieved via the Binder parameter defined as follows

$$g_L = \frac{1}{2}\left(3 - \frac{[\langle q^4\rangle]_{\mathrm{av}}}{[\langle q^2\rangle]_{\mathrm{av}}^2}\right). \tag{15}$$

Here $\langle q^2\rangle$ and $\langle q^4\rangle$ are, respectively, the second and the fourth cumulant moment of q. In this calculation, in order to avoid systematic correlation errors that could bias the results if we were evaluating this average over g_L directly,[35] the second and fourth order cumulants are averaged prior to taking their ratio. The Binder parameter is constrained in the range $0 \leqslant g_L \leqslant 1$. At high temperature, where thermal fluctuations overcome all cooperative interaction, the system is expected to exist in the paramagnetic phase where there is no spatial autocorrelation. As a result, the distribution of q should be Gaussian centered at $q=0$. In this case the ratio of the cumulants, $\langle q^4\rangle/\langle q^2\rangle^2 \to 3$, resulting in $g_L \to 0$. At low temperatures, the cooperative interaction becomes dominant and the ratio of the cumulants approaches unity so that $g_L \to 1$.

Figure 6 (inset) displays the temperature dependence of the Binder parameter for a variety of network sizes. A spin-glass state is observed for lower temperatures where the Binder parameter deviates from zero, and increases with the system size while approaching to 1. In the thermodynamic limit, we expect $g_L \to 1$ just below the critical temperature. A crossing point in the size dependence of g_L indicates that the critical temperature for the SG phase transition is $T \sim 4.0$. Figure 6 indicates that for temperatures above $T \sim 4.0$ the Binder parameter, while remaining always above zero, does indeed order in an opposite manner indicative of a genuine crossing of the curves and in accord with a genuine spin glass transition at finite temperature. This feature is not observed for uniformly distributed AF and FM bonds, as

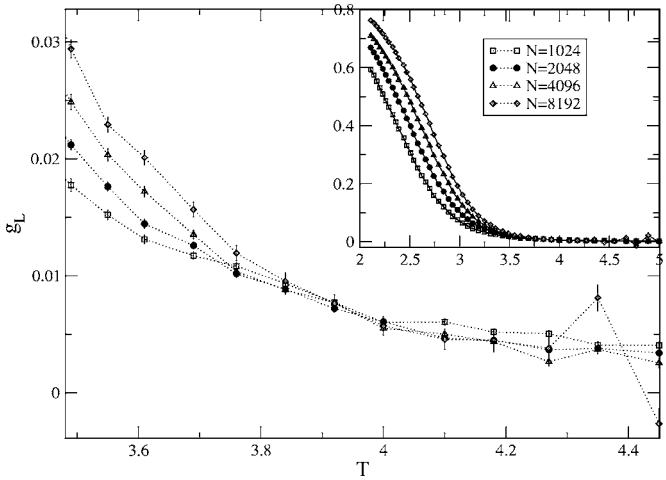

FIG. 6. Scaling behavior of the Binder cumulant, g_L, for different system sizes. Each system size is averaged over 1000 realizations of the network configuration.

$T_c=\infty$ in the thermodynamic limit.[24] However, the value of the transition temperature is not determined with high accuracy by the crossing of the Binder parameter. In fact, finite size effects seem to slightly distort the tendency for very small networks, as in the case of $N=1024$. At the same time, the statistical errors in the paramagnetic phase for large networks, see $N=8192$, appear to be significant and some points are scattered.

A more accurate estimate of the critical temperature, T_c, for finite size systems can be obtained using scaling arguments. For a SG system, the Binder parameter depends on the system size L as

$$g_L = \tilde{g}_L[(T - T_c)L^{1/\nu}], \tag{16}$$

$\nu>0$ being the spin-glass correlation length exponent, implying that at T_c the Binder cumulant does not depend on L. For the SFN, the system size scales logarithmically with the number of nodes N[16–18,24] and therefore we take $L=\log(N)$. This slow increase in the diameter of the system, as well as the average path length, is a manifestation of the "small-world" property of this network, induced by the presence of a large number of highly connected hubs which create shortcuts between the nodes. An important implication of this feature is that we cannot embed the network in any finite dimensional lattice: we are implicitly dealing with a high dimensional system. The correlation length, in this case, is still well-defined although its value gets close to the densely connected, mean field limit as we increase the average connectivity of the nodes, $\langle k\rangle=2m$.

The parameters T_c and ν are determined by constraining the temperature dependence of the Binder parameter for each network size to lie on a single curve. The curves following the scaling bahavior of Eq. (16) are shown in Fig. 7. From this fit we estimate the critical temperature $T_c\sim 4.0(1)$ and the exponent of the SG correlation length $\nu\sim 1.10(2)$. It is important to underline that this kind of behavior is not observed for an AF system on a regular triangular lattice.

IV. CONCLUDING REMARKS

In summary, we have investigated the antiferromagnetic Ising model on a Barabási-Albert scale-free network using the replica exchange Monte Carlo method. Through the calculation of the overlap parameter we observe spin-glass behavior at low temperatures. Using the scaling behavior of the Binder parameter the critical temperature separating the SG and the paramagnetic phases is found to be $T_c=4.0(2)$ with a scaling exponent of SG correlation length $\nu\sim 1.10(2)$. Such behavior is not observed for the AF Ising model on regular triangular lattices. Hence the topology of the interactions plays a critical role in the dynamics of the system.

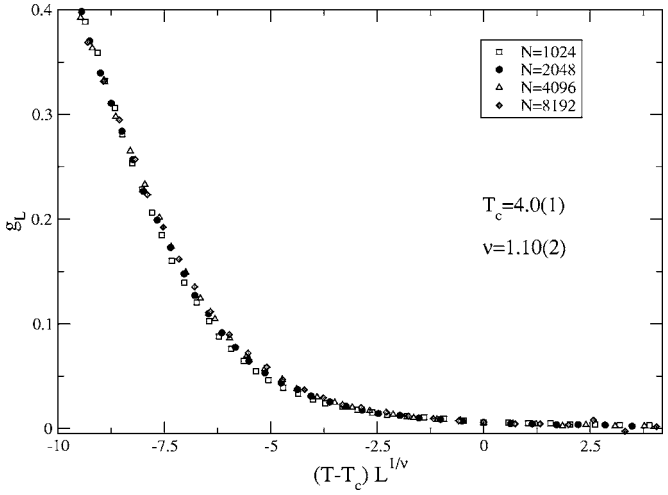

FIG. 7. Scaling plot of the data illustrated in Fig. 6, fitted to Eq. (16).

ACKNOWLEDGMENTS

The authors wish to thank Y. Okabe, E. Marinari, and J.-S. Wang for valuable discussions. One of the authors (T.S.) is grateful for the hospitality of the Center for the Subatomic Structure of Matter (CSSM) at the University of Adelaide during his academic visit to the Center. The computation of this work has been done using the Hydra teraflop supercomputer facility of the South Australian Partnership for Advanced Computing (SAPAC).

*Electronic address: mbartolo@physics.adelaide.edu.au
†Electronic address: tasrief@unhas.ac.id
‡Electronic address: dleinweber@physics.adelaide.edu.au
§Electronic address: anthony.williams@adelaide.edu.au

[1] R. J. Williams, E. L. Berlow, J. A. Dunne, A.-L. Barabási, and W. D. Martinez, Proc. Natl. Acad. Sci. U.S.A. **99**, 12913 (2002); J. Camacho, R. Guimerà, and L. A. N. Amaral, Phys. Rev. Lett. **88**, 228102 (2002); J. M. Montoya and R. V. Solé, J. Theor. Biol. **214**, 405 (2002).

[2] L. A. N. Amaral, A. Scala, M. Barthelemy, and H. E. Stanley, Proc. Natl. Acad. Sci. U.S.A. **97**, 11 (2000).

[3] D. J. Watts and S. H. Strogatz, Nature (London) **393**, 440 (1998).

[4] H. Jeong, B. Tombor, R. Albert, Z. N. Oltvai, and A.-L. Barabási, Nature (London) **407**, 651 (2000); H. Jeong, S. P. Mason, Z. N. Oltvai, and A.-L. Barabási, *ibid.* **411**, 41 (2001).

[5] F. Liljeros, C. R. Edling, L. A. N. Amaral, H. E. Stanley, and Y. Aberg, Nature (London) **411**, 907 (2001).

[6] M. Faloutsos, P. Faloutsos, and C. Faloutsos, Comput. Commun. Rev. **29**, 251 (1999); R. Pastor-Satorras, A. Vazquez, and A. Vespignani, Phys. Rev. Lett. **87**, 258701 (2001); S. Yook, H. Jeong, and A.-L. Barabási, Proc. Natl. Acad. Sci. U.S.A. **99**, 13382 (2002).

[7] R. Albert, H. Jeong, and A.-L. Barabási, Nature (London) **401**, 130 (1999); R. Kumar, P. Raghavan, S. Rajagopalan, D. Sivakumar, A. Tomkins, and E. Upfal, *Proceedings of the 9th ACM Symposium on Principles of Database Systems* (ACM Press,

New York, 2000), p. 1.
[8] M. E. J. Newman, S. H. Strogatz, and D. J. Watts, Phys. Rev. E **64**, 026118 (2001); R. Albert and A.-L. Barabási, Phys. Rev. Lett. **85**, 5234 (2000).
[9] A.-L. Barabási and R. Albert, Science **286**, 509 (1999).
[10] S. Redner, Eur. Phys. J. B **4**, 131 (1998); A. Vasquez, Europhys. Lett. **54**, 430 (2001).
[11] G. Bonanno, G. Caldarelli, F. Lillo, and R. N. Mantegna, Phys. Rev. E **68**, 046130 (2003); J.-P. Onnela, A. Chakraborti, K. Kaski, J. Kertesz, and A. Kanto, *ibid.* **68**, 056110 (2003).
[12] B. Bollobás, *Random Graphs*, 2nd ed. (Cambridge University Press, Cambridge, 2001).
[13] R. Pastor-Satorras and A. Vespignani, Phys. Rev. Lett. **86**, 3200 (2001); *ibid.* **63**, 066117 (2001).
[14] M. Bartolozzi, D. B. Leinweber, and A. W. Thomas, Phys. Rev. E **72**, 046113 (2005).
[15] R. Albert, H. Jeong, and A.-L. Barabási, Nature (London) **406**, 378 (2000); R. Cohen, K. Erez, D. ben-Avraham, and S. Havlin, Phys. Rev. Lett. **85**, 4626 (2000); D. S. Callaway, M. E. J. Newman, S. H. Strogatz, and D. J. Watts, *ibid.* **85**, 5468 (2000).
[16] R. Albert and A.-L. Barabási, Rev. Mod. Phys. **74**, 47 (2002).
[17] S. N. Dorogovtsev and J. F. F. Mendes, Adv. Phys. **51**, 1079 (2002).
[18] S. N. Dorogovtsev and J. F. F. Mendes, *Evolution of Networks* (Oxford University Press, Oxford, 2003).
[19] S. N. Dorogovtsev, A. V. Goltsev, and J. F. F. Mendes, Phys. Rev. E **66**, 016104 (2002).
[20] F. Iglói and L. Turban, Phys. Rev. E **66**, 036140 (2002).
[21] A. Aleksiejuk, J. A. Holyst, and D. Stauffer, Physica A **310**, 260 (2002).
[22] C. P. Herrero, Phys. Rev. E **69**, 067109 (2004).
[23] K. Binder and A. P. Young, Rev. Mod. Phys. **58**, 801 (1986); N. Kawashima and H. Rieger, in *Frustrated Spin Systems*, edited by H.-T. Diep (World Scientific, Singapore, 2004).
[24] D.-H. Kim, G. J. Rodgers, B. Kahng, and D. Kim, Phys. Rev. E **71**, 056115 (2005).
[25] P. Holme and B. J. Kim, Phys. Rev. E **65**, 026107 (2002).
[26] K. Hukushima and K. Nemoto, J. Phys. Soc. Jpn. **65**, 1863 (1996).
[27] Download at http://vlado.fmf.uni-lj.si/pub/networks/pajek/
[28] R. F. S. Andrade and H. J. Herrmann, Phys. Rev. E **71**, 056131 (2005).
[29] T. Surungan, Y. Okabe, and Y. Tomita, J. Phys. A **37**, 4219 (2004).
[30] S. F. Edwards and P. W. Anderson, J. Phys. F: Met. Phys. **5**, 965 (1975).
[31] G. Parisi, Phys. Rev. Lett. **50**, 1946 (1983).
[32] R. N. Bhatt and A. P. Young, Phys. Rev. B **37**, 5606 (1988).
[33] A. T. Ogielski, Phys. Rev. B **32**, 7384 (1985).
[34] V. Dotsenko, *Introduction to the Replica Theory of Disordered Statistical Systems* (Cambridge University Press, Cambridge, 2001).
[35] N. Kawashima and A. P. Young, Phys. Rev. B **53**, R484 (1996).